Available online at www.sciencedirect.com
SCIENCE DIRECT®
Biochemical Pharmacology 65 (2003) 1957–1965
Biochemical Pharmacology
www.elsevier.com/locate/biochempharm

Metabolism of 26,26,26,27,27,27-F_6-1α,25-dihydroxyvitamin D_3 by CYP24: species-based difference between humans and rats

Toshiyuki Sakaki[a,*], Natsumi Sawada[a], Daisuke Abe[a], Koichiro Komai[b], Shunichi Shiozawa[b], Yasuki Nonaka[c], Kimie Nakagawa[d], Toshio Okano[d], Miho Ohta[e], Kuniyo Inouye[a]

[a]*Division of Food Science and Biotechnology, Graduate School of Agriculture, Kyoto University, Kitashirakawa, Oiwake-cho, Sakyo-ku, Kyoto 606-8502, Japan*
[b]*Faculty of Health Science, Kobe University School of Medicine 7-10-2, Tomogaoka, Suma-ku, Kobe 654-0142, Japan*
[c]*College of Nutrition, Koshien University, Takarazuka, Hyogo 665-0006, Japan*
[d]*Department of Hygienic Sciences, Kobe Pharmaceutical University, Kobe 658-8558, Japan*
[e]*Laboratory of Nutrition, Koshien College, 4-25 Kawarabayashi-cho, Nishinomiya 663-8107, Japan*

Received 10 July 2002; accepted 25 February 2003

Abstract

The compound 26,26,26,27,27,27-F_6-1α,25$(OH)_2D_3$ is a hexafluorinated analog of the active form of Vitamin D_3. The enhanced biological activity of F_6-1α,25$(OH)_2D_3$ is considered to be related to a decreased metabolic inactivation of the compound in target tissues such as the kidneys, small intestine, and bones. Our previous study demonstrated that CYP24 is responsible for the metabolism of F_6-1α,25$(OH)_2D_3$ in the target tissues. In this study, we compared the human and rat CYP24-dependent metabolism of F_6-1α,25$(OH)_2D_3$ by using the *Escherichia coli* expression system. In the recombinant *E. coli* cells expressing human CYP24, bovine adrenodoxin and NADPH-adrenodoxin reductase, F_6-1α,25$(OH)_2D_3$ was successively converted to F_6-1α,23*S*,25$(OH)_3D_3$, F_6-23-oxo-1α,25$(OH)_2D_3$, and the putative ether compound with the same molecular mass as F_6-1α,25$(OH)_2D_3$. The putative ether was not observed in the recombinant *E. coli* cells expressing rat CYP24. These results indicate species-based difference between human and rat CYP24 in the metabolism of F_6-1α,25$(OH)_2D_3$. In addition, the metabolite with a cleavage at the C_{24}–C_{25} bond of F_6-1α,25$(OH)_2D_3$ was detected as a minor metabolite in both human and rat CYP24. Although F_6-1α,23*S*,25$(OH)_3D_3$ and F_6-23-oxo-1α,25$(OH)_2D_3$ had a high affinity for Vitamin D receptor, the side-chain cleaved metabolite and the putative ether showed extremely low affinity for Vitamin D receptor. These findings indicate that human CYP24 has a dual pathway for metabolic inactivation of F_6-1α,25$(OH)_2D_3$ while rat CYP24 has only one pathway. Judging from the fact that metabolism of F_6-1α,25$(OH)_2D_3$ in rat CYP24-harboring *E. coli* cells is quite similar to that in the target tissues of rat, the metabolism seen in human CYP24-harboring *E. coli* cells appear to exhibit the same metabolism as in human target tissues. Thus, this recombinant system harboring human CYP24 appears quite useful for predicting the metabolism and efficacy of Vitamin D analogs in human target tissues before clinical trials.

Keywords: Metabolism of Vitamin D; Vitamin D analog; CYP24; Hexafluoro-1α,25-dihydroxyvitamin D_3; Cytochrome P450; Species-based difference

1. Introduction

Vitamin D analogs are potentially useful for clinical treatments of type I rickets, osteoporosis, renal osteodystrophy, psoriasis, leukemia and breast cancer [1,2]. On the metabolism of Vitamin D analogs, the metabolism intarget tissues such as the kidneys, the small intestine and bones is pharmacologically essential as reported by Komuro *et al*. [3–5]. 26,26,26,27,27,27-Hexafluoro-1α,25$(OH)_2D_3$, which is now clinically used as a drug for secondary hyperparathyroidism, has been reported to be several times more potent than the parent compound at increasing intestinal calcium transport and bone calcium mobilization in Vitamin D-deficient rats fed a low-calcium diet and at directly stimulating alkaline phosphatase activity in bone derived cells [6–8]. The reason for enhanced biologic activity in the kidneys and the small intestine appears to be related to F_6-1α,25$(OH)_2D_3$

* Corresponding author. Tel.: +81-75-753-6267; fax: +81-75-753-6265.
E-mail address: tsakaki@kais.kyoto-u.ac.jp (T. Sakaki).
Abbreviations: P450 CYP, cytochrome P450; 1α,25$(OH)_2D_3$, 1α,25-dihydroxyvitamin D_3; F_6-1α,25$(OH)_2D_3$, 26,26,26,27,27,27-hexafluoro-1α,25-dihydroxyvitamin D_3; VDR, Vitamin D receptor.

0006-2952/03/$ – see front matter
doi:10.1016/S0006-2952(03)00190-4

metabolism to 26,26,26, 27,27,27-hexafluoro-1α,23*S*,25-$(OH)_3D_3$, a bioactive 23*S*-hydroxylated form that is resistant to further metabolism [9,10].

Recently, we revealed enzymatic properties of human 25-hydroxyvitamin D_3 ($25(OH)D_3$) 24-hydroxylase (CYP24) expressed in *Escherichia coli* cells [11]. Human CYP24 demonstrated a remarkable metabolism consisting of both C-23 and C-24 hydroxylation pathways towards $25(OH)D_3$ and $1\alpha,25(OH)_2D_3$. The molar ratio of metabolites between C-23 and C-24 hydroxylation pathways was approximately 1:4. However, rat CYP24 showed only C-24 hydroxylation pathway [12]. Extreme predominance of C-24 over C-23 pathways was also demonstrated in mouse CYP24 [13]. On the other hand, most of the metabolites observed in guinea pig were included in C23-hydroxylation pathway [14]. These facts mean that the preclinical tests using animals such as rat, mouse and guinea pig would not correctly predict the metabolism of Vitamin D analogs in human body.

As described previously [11,12,15–17], *E. coli* expression system has low backgrounds on kinetic studies of P450 relating to the metabolism of Vitamin D_3 because of the absence of a P450 gene in *E. coli* genome [18] and no steroids in *E. coli* cell membrane. We can readily obtain the metabolites of Vitamin D and Vitamin D analogs using the recombinant living cells. In this report, we compare human CYP24-dependent metabolism of F_6-$1\alpha,25(OH)_2D_3$ with rat CYP24-dependent metabolism using co-expression system consisting of CYP24, adrenodoxin (ADX), and NADPH-adrenodoxin reductase (ADR).

2. Materials and methods

2.1. Materials

DNA modifying enzymes, restriction enzymes and DNA sequencing kit were purchased from Takara Shuzo Co, Ltd. *E. coli* JM109 (Takara Shuzo Co) was used as a host strain. F_6-$1\alpha,25(OH)_2D_3$, F_6-$1\alpha,23S,25(OH)_3D_3$ and F_6-23-oxo-$1\alpha,25(OH)_2D_3$, 1β-epimer, 3α-epimer, 1β-3α-epimer of F_6-$1\alpha,25(OH)_2D_3$, and F_6-$1\alpha,24R(OH)_2D_3$ were generous gifts from Sumitomo Pharmaceuticals. $1\alpha,25(OH)_2D_3$ was purchased from Solvey–Dupher Co. [26,27-Methyl-^{3}H]$1\alpha,25(OH)_2D_3$ (specific activity: 6.7 TBq $mmol^{-1}$) was purchased from Amersham Co. NADPH was purchased from Oriental Yeast Co. Terrific broth was purchased from Gibco BRL. Other chemicals used were of the highest quality commercially available.

2.2. Construction of expression plasmids

The expression plasmids, pKSN24R2 for mature form of rat CYP24, and pKH24 for mature form of human CYP24 were constructed as described [11,15] (Fig. 1). The co-expression plasmid pK24XR for mature forms of human CYP24, bovine ADX, and NADPH-ADR was constructed as described previously [19]. The cDNAs encoding mature forms of human CYP24, bovine ADX, and bovine ADR each containing a ribosomal-binding sequence were organized into a polycistronic transcription unit under the regulation of *tac* promoter [11]. The co-expression plasmid pKSN24XR for mature forms of rat CYP24, bovine ADX, and NADPH-ADR was constructed as follows. The plasmid pKSN24R2 was partially digested with Hind III, and ligated with the Hind III fragment containing coding region of mature forms of bovine ADX and ADR obtained from the plasmid pKAXR [17].

2.3. Cultivation of the recombinant E. coli cells

Recombinant *E. coli* cells were grown in Terrific broth containing 50 μg mL^{-1} ampicillin at 26° under good aeration. The induction of transcription of 24-hydroxylase cDNA under the *tac* promoter was initiated by addition of isopropyl-thio-β-D-galactopyranoside at a final concentration of 1 mM when the cell density (OD 660) reached 0.5. δ-Aminolevulinic acid was also added at a final concentration of 0.5 mM simultaneously. The recombinant cells were gently shaken at 26° under good aeration by bubbling.

2.4. Measurement of reduced CO difference spectra and substrate-induced difference spectra

The absorption-coefficient difference between 445 and 490 nm ($\Delta\varepsilon_{445-490}$) = 105 mM^{-1} cm^{-1} was used for the calculation of the P450 hemoprotein concentration, as described previously [15]. The substrate-induced difference spectra of the membrane fraction were measured in the presence of 0–2.0 μM of $1\alpha,25(OH)_2D_3$ or F_6-$1\alpha,25(OH)_2D_3$.

2.5. Measurement of enzyme activity of CYP24

Metabolism of F_6-$1\alpha,25(OH)_2D_3$, F_6-$1\alpha,23S,25(OH)_3D_3$, and F_6-23-oxo-$1\alpha,25(OH)_2D_3$ was measured in the reconstituted system containing the membrane fraction prepared

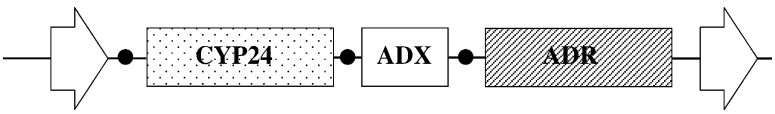

Fig. 1. Structure of co-expression plasmids for rat CYP24 or human CYP24 with bovine ADX and ADR. The shaded, open and striped boxes indicate the coding regions of CYP24, ADX, and ADR, respectively. The arrows indicate *tac* promoter and *rrnB* terminator. The closed circles indicate ribosomal binding sites.

from the recombinant *E. coli* cells containing 0.01–0.02 μM of CYP24, 5.0 μM of ADX, 0.5 μM of NADPH-ADR, 0–10.0 μM of the substrate, 0.5 mM of NADPH, 100 mM Tris–HCl pH 7.4, and 1 mM EDTA at 37° as described previously [10]. The reaction was initiated by addition of NADPH. Aliquots of the reaction mixture were collected after varying time-intervals and extracted with 4 vol. of chloroform–methanol (3:1). The organic phase was recovered and dried up. The resultant residue was solubilized with acetonitrile, and applied to HPLC under the following conditions: column, YMC-Pack ODS-AM (4.6 mm× 300 mm) (YMC Co); UV detection, 265 nm; flow-rate, 1.0 mL min^{-1}; column temperature, 40°; mobile phase, acetonitrile:water (50:50, v/v) for 5 min followed by a linear gradient of 50–100% acetonitrile aqueous solution per 15 min and 100% acetonitrile for 10 min.

In the case of living cells, each of the substrates, F_6-1α,25$(OH)_2D_3$, F_6-1α,23*S*,25$(OH)_3D_3$, and F_6-23-oxo-1α,25$(OH)_2D_3$ 25$(OH)D_3$ in ethanol solution was added at a final concentration of 5.0 μM into the cell culture. After 30 min, isopropyl-thio-β-D-galactopyranoside was added at a final concentration of 1 mM. Aliquots of the cell culture were collected after varying time-intervals, and extracted with 4 vol. of chloroform–methanol (3:1).

2.6. LC-MS analysis of the metabolites

Isolated metabolites from HPLC effluents were subjected to mass spectrometric analysis using a Finnegan mat TSQ-70 with atmospheric pressure chemical ionization, positive mode. The conditions of LC were described below: column; reverse phase ODS column (6 mm × 150 mm) (μBondapak C18, Waters); mobile phase, 80% methanol aqueous solution per 25 min; flow-rate, 1.0 mL min^{-1}; UV detection, 265 nm.

2.7. GC-MS analysis of TMS-derivatives of the metabolites

The authentic standard of F_6-1α,25$(OH)_2D_3$, F_6-1α,23*S*,25$(OH)_3$, and 23-oxo-F_6-1α,25$(OH)_2D_3$, and the metabolite M3 were each trimethylsilylated in *N*,*O*-bis(trimethylsilyl)trifluoroacetamide containing 5% trimethylchlorosilane and 10% pyridine and 5% trimethylchlorosilane at 55° for 1 hr. GC-MS analysis was performed using a Finnigan Mat Thermo quest GC with EI mode. The capillary column BPX5 (0.25 mm × 30 m) (SGE International Co) was used as a GC column with a temperature program raging 100–300°.

2.8. Binding assay for calf-thymus Vitamin D receptor

Displacement of [^{3}H]-1α,25$(OH)_2D_3$ from calf-thymus cytosol receptor (Yamasa Shoyu) by 1α,25$(OH)_2D_3$ or metabolites of F_6-1α,25$(OH)_2D_3$ was determined as described previously [20]. The increasing amounts of 1α,25$(OH)_2D_3$ (0.0156–128 pg) or the metabolites (0.25–16,384 pg) in 20 μL ethanol were added to 500 μL of the calf-thymus cytosol diluted with 50 mM potassium phosphate buffer (pH 7.4) containing 0.3 M KCl, and incubated for 1 hr at 20°. Next, 34 fmol of [^{3}H]-1α,25$(OH)_2D_3$ in 25 μL ethanol was added and incubated for 1 hr at 20°. The 200 μL of dextran–charcoal (0.05% dextran T-150, 0.5% Charcoal Decolorizing Neutral) in 50 mM sodium phosphate buffer (pH 7.5), which was freshly prepared and stirred well before addition, was added to separate bound and free [^{3}H]-1α,25$(OH)_2D_3$. The assay tube was shaken with a vortex mixer and centrifuged at 1000 *g* for 10 min at 4°. The radioactivity in the supernatant was measured with a liquid scintillation counter.

2.9. Other methods

The concentrations of Vitamin D_3 derivatives were estimated by their molar extinction coefficient of 1.80×10^4 M^{-1} cm^{-1} at 264 nm [21]. Protein concentration was determined by the method of Lowry *et al.* [22], using bovine serum albumin as a standard.

3. Results

3.1. Expression of human CYP24 in E. coli

Membrane fraction was prepared from the recombinant *E. coli* JM109/pKH24 cells for human CYP24, and JM109/pKSN24R2 cells for rat CYP24. The human CYP24 and rat CYP24 contents in the membrane fractions were calculated to be 76 and 82 pmol mg^{-1} protein, respectively.

3.2. Substrate-induced spectra of human and rat CYP24

The addition of 1α,25$(OH)_2D_3$ or F_6-1α,25$(OH)_2D_3$ to the membrane fraction containing human or rat CYP24 induced a typical type I spectrum (data not shown), indicating a change of the heme iron of the CYP24 from a low-spin state to a high-spin state upon the substrate binding.

3.3. CYP24-dependent activity in reconstituted system

The reconstituted system containing the membrane fraction prepared from the recombinant *E. coli* cells, ADX and ADR was examined for the metabolism of the substrates F_6-1α,25$(OH)_2D_3$, F_6-1α,23*S*,25$(OH)_3D_3$, and F_6-23-oxo-1α,25$(OH)_2D_3$. On the metabolism of F_6-1α,25$(OH)_2D_3$, both human CYP24 and rat CYP24 showed a metabolite at the same retention time as F_6-1α,23*S*,25$(OH)_3D_3$. On the metabolism of F_6-1α,23*S*,25$(OH)_3D_3$, both CYP24 species showed only trace amount of metabolite at the same retention time as F_6-23-oxo-1α,25$(OH)_2D_3$ (data not shown).

However, no detectable metabolites towards F_6-23-oxo-1α,25$(OH)_2D_3$ were observed in both CYP24 species. These results suggest that both human and rat CYP24 catalyze the conversion from F_6-1α,25$(OH)_2D_3$ via F_6-1α,23*S*,25$(OH)_3D_3$ to F_6-23-oxo-1α,25$(OH)_2D_3$, although second reaction rate is much lower than the first reaction rate.

3.4. Determination of K_m and V_{max} values for 23S-hydroxylation towards F_6-1α,25$(OH)_2D_3$

When the 23*S*-hydroxylation activity towards F_6-1α,25$(OH)_2D_3$ was measured at the substrate concentrations of 0.1–1.0 μM, the reaction followed Michaelis–Menten type kinetics. The K_m and V_{max} values for human CYP24 determined with Hanes–Woolf plots were 0.063± 0.029 μM and 0.45 ± 0.09 mol min^{-1} mol^{-1} P450. On the other hand, the K_m and V_{max} values for rat CYP24 were estimated to be 0.056 ± 0.017 μM and 0.20± 0.01 mol min^{-1} mol^{-1} P450. Thus, the physiologically essential parameter V_{max}/K_m value for human CYP24 was 2-fold higher than the V_{max}/K_m value for rat CYP24.

3.5. CYP24-dependent activity in living cell

The substrate F_6-1α,25$(OH)_2D_3$ was added to cell culture of the recombinant *E. coli* cells. Aliquots of the cell culture were collected after varying time-intervals and extracted with chloroform–methanol (3:1) and analyzed with HPLC (Fig. 2). The metabolites were detected in the time-dependent manner in the recombinant cells expressing CYP24, but not in the control JM109/pKSNdl cells. In JM109/pK24XR cells expressing human CYP24, bovine ADX, and bovine ADR, a major metabolite (M1) was observed at the same retention time as F_6-1α,23*S*,25$(OH)_3D_3$. As shown in Fig. 3, the metabolite showed the molecular ion at *m/z* 541 (M + H), and fragment ions at 523 (541-H_2O), 505 (541-2H_2O), 379 (433-3H_2O), and 361 (433-4H_2O). The spectrum coincided with that of authentic standard of F_6-1α,23*S*,25$(OH)_3D_3$. These results strongly suggest that M1 is F_6-1α,23*S*,25$(OH)_3D_3$. The second major metabolite (M2) was observed at the same retention time as F_6-1α,23*S*,25$(OH)_3D_3$. The mass spectrum of the metabolite shown in Fig. 3 also suggests that M2 is F_6-23-oxo-1α,25$(OH)_2D_3$. Furthermore, F_6-23-oxo-1α,25$(OH)_2D_3$ was detected in the early stage of the cultivation when total conversion rate (%) of metabolites was less than 20% (Fig. 4). In addition to these metabolites, two novel metabolites designated as M3 and M4 were observed. Here, the mass spectrum of M3 is quite similar to F_6-1α,25$(OH)_3D_3$ (Fig. 3) Thus, it was assumed that M3 was an epimer of F_6-1α,25$(OH)_2D_3$. However, the HPLC retention time of M3 (22.1 min) was different from the 1β-epimer (21.9 min),

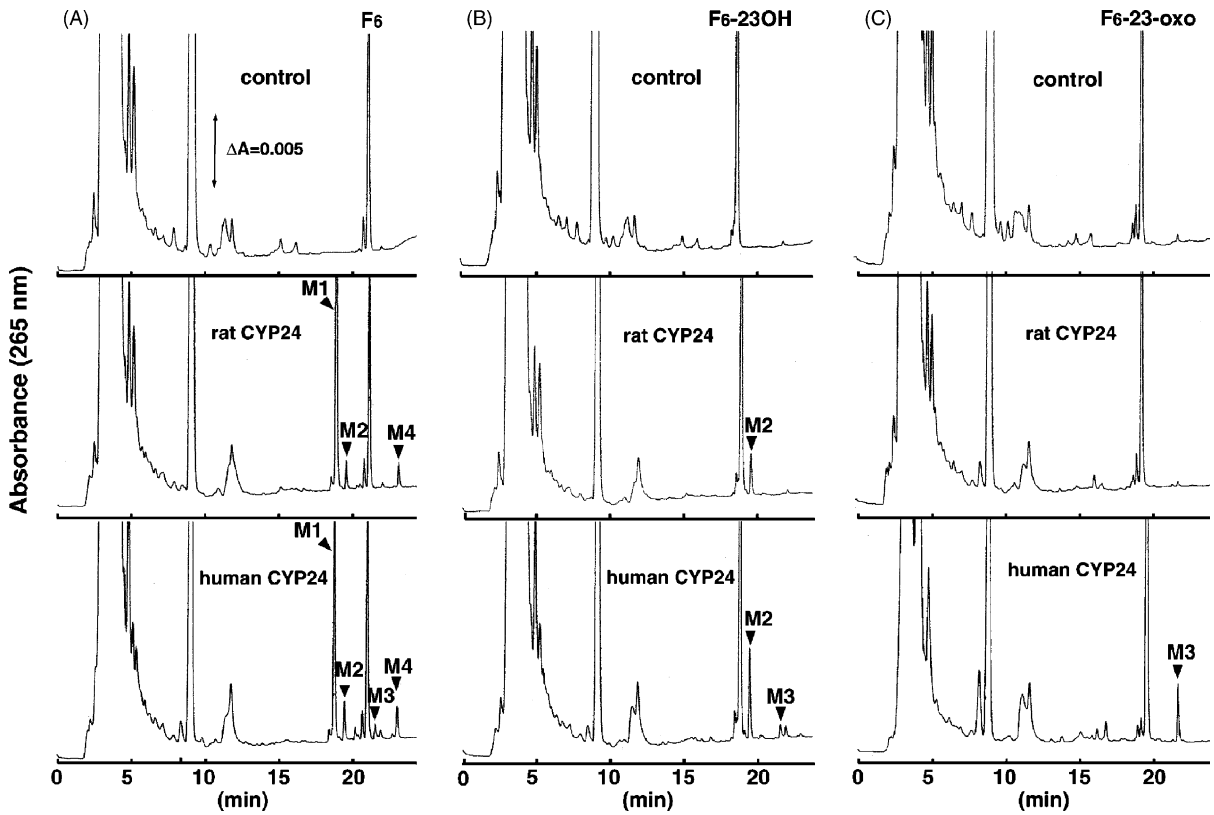

Fig. 2. HPLC profiles of F_6-1α,25$(OH)_2D_3$ (A), F_6-1α,23*S*,25$(OH)_3D_3$ (B), F_6-23-oxo-1α,25$(OH)_2D_3$ (C) and their metabolites extracted from whole cell cultures of the recombinant *E. coli* JM109/pKSNdl (control), JM109/pK24XR (rat CYP24) and JM109/pKH24XR (human CYP24). Following 39 hr of cultivation with the substrate, each whole cell culture was extracted and analyzed by HPLC. F_6, F_6-23OH and F_6-23-oxo indicate F_6-1α,25$(OH)_2D_3$, F_6-1α,23*S*,25$(OH)_3D_3$ and F_6-23-oxo-1α,25$(OH)_2D_3$, respectively. The experiments were repeated three times.

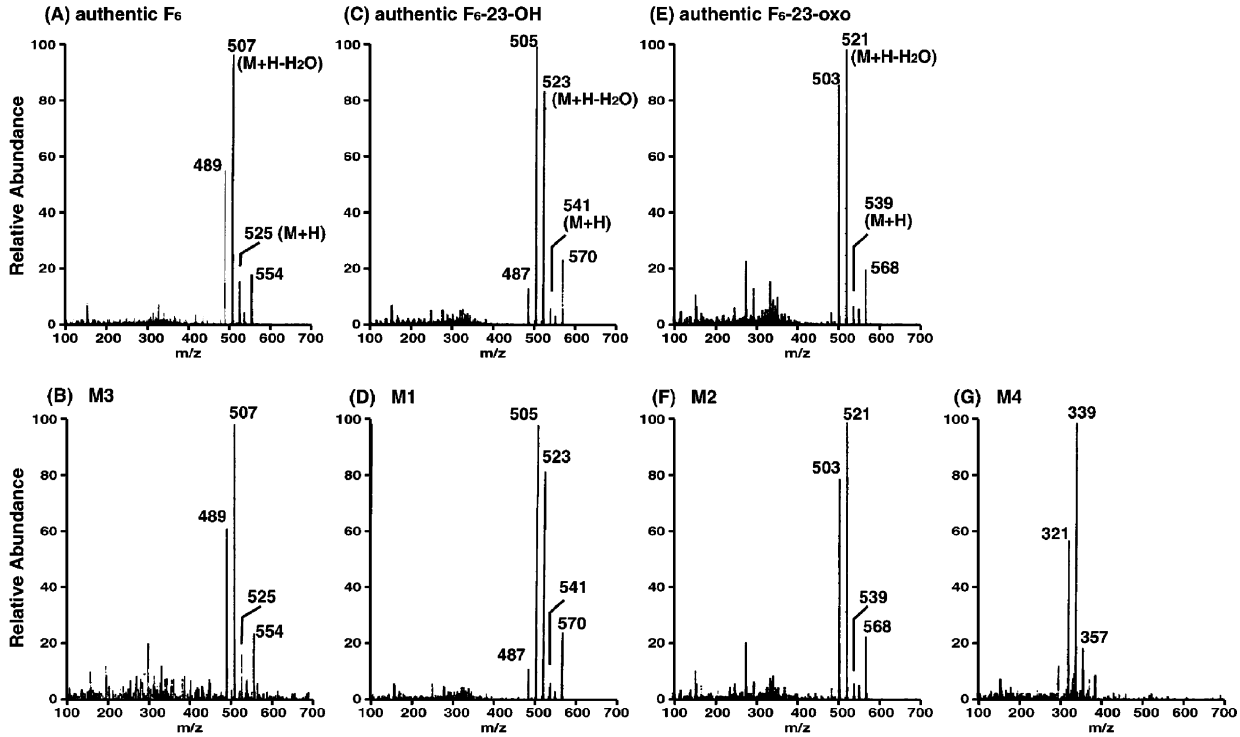

Fig. 3. Mass spectra of authentic F_6-1α,25$(OH)_2D_3$ (A), the metabolite M3 (B), F_6-1α,23*S*,25$(OH)_3D_3$ (C), the metabolite M1 (D), authentic F_6-23-oxo-1α,25$(OH)_2D_3$ (E), M2 (F) and M4 (G) shown in Fig. 2. The metabolites were extracted from the recombinant *E. coli* cells harboring human CYP24, isolated by HPLC, and then analyzed by mass spectrometry as described in Section 2. F_6, F_6-23OH and F_6-23-oxo indicate F_6-1α,25$(OH)_2D_3$, F_6-1α,23*S*,25$(OH)_3D_3$ (B), F_6-23-oxo-1α,25$(OH)_2D_3$, respectively. The experiments were repeated twice.

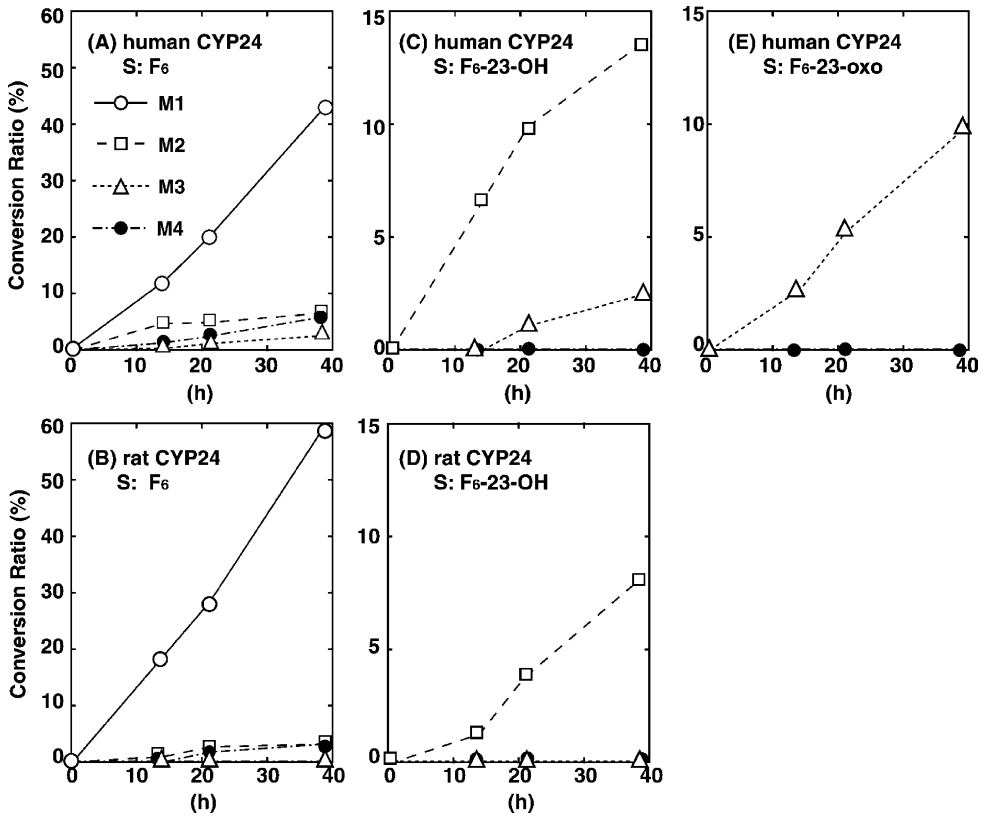

Fig. 4. Time courses of metabolism of F_6-1α,25$(OH)_2D_3$ by human CYP24 (A), F_6-1α,25$(OH)_2D_3$ by rat CYP24 (B), F_6-1α,23*S*,25$(OH)_3D_3$ by human CYP24 (C), F_6-1α,23*S*,25$(OH)_3D_3$ by rat CYP24 (D), and F_6-23-oxo-1α,25$(OH)_2D_3$ by human CYP24 (E). Conversion ratios from the substrate to the indicated metabolites were estimated based on HPLC analysis. The metabolites M1 to M4 correspond to those in Fig. 2. The experiments were repeated three times.

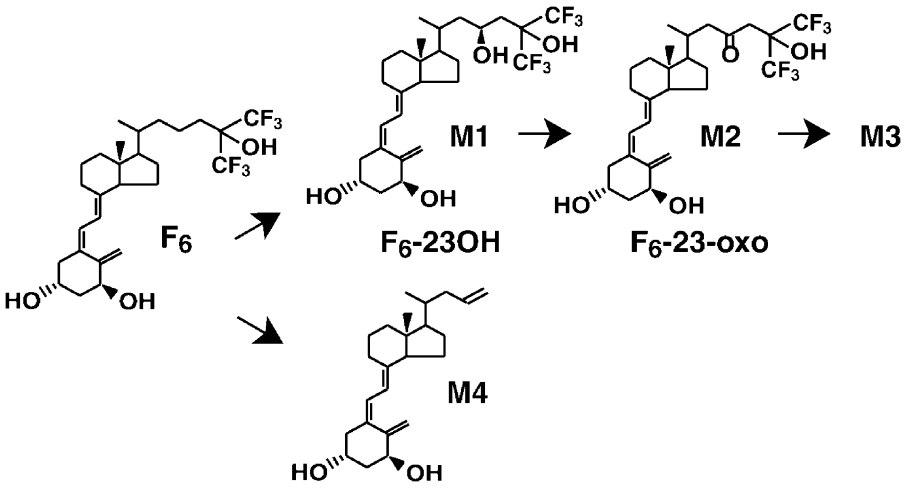

Fig. 5. Human CYP24-dependent metabolic pathways of F_6-1α,25$(OH)_2D_3$. The conversion from F_6-23-oxo-1α,25$(OH)_2D_3$ to the putative ether of F_6-1α,25$(OH)_2D_3$ (M3) was observed in human CYP24-dependent metabolism, but not observed in rat CYP24-dependent one. F_6, F_6-23OH and F_6-23-oxo indicate F_6-1α,25$(OH)_2D_3$, F_6-1α,23*S*,25$(OH)_3D_3$ and F_6-23-oxo-1α,25$(OH)_2D_3$, respectively.

3α-epimer (21.7 min), 1β-3α-epimer (21.5 min), and F_6-1α,24*R*$(OH)_2D_3$ (19.9 min) examined in this study. On the other hand, the molecular ion at 357, and fragment ions at 339 and 321 of the metabolite M4 were assumed to be those for (M + H), (M + H-H_2O), and (M + H-2H_2O), suggesting that M4 was produced by side-chain cleavage at the C_{24}–C_{25} bond of F_6-1α,25$(OH)_2D_3$ (Fig. 3). In JM109/pKSN24XR cells expressing rat CYP24, bovine ADX and ADR, F_6-1α,23*S*,25$(OH)_3D_3$ was detected as a major metabolite as in the case of JM109/pK24XR cells. The conversion ratio to F_6-23-oxo-1α,25$(OH)_2D_3$ was significantly lower than that in JM109/pK24XR cells. Although the metabolite M4 was observed, M3 was not observed up to 39 hr of the cultivation. These results indicate species-based difference on the CYP24-dependent metabolism of F_6-1α,25$(OH)_2D_3$ between humans and rats.

A significant difference was also observed in the metabolism of F_6-1α,23*S*,25$(OH)_3D_3$. In the recombinant *E. coli* cells expressing rat CYP24, only F_6-23-oxo-1α,25$(OH)_2D_3$ was observed as a metabolite. On the other hand, human CYP24 showed two metabolites: F_6-23-oxo-1α,25$(OH)_2D_3$ and M3. The time course of conversion ratio of the two metabolites suggested that M3 was produced from F_6-1α,23*S*,25$(OH)_3D_3$ via F_6-23-oxo-1α,25$(OH)_2D_3$. To confirm this assumption, F_6-23-oxo-1α,25$(OH)_2D_3$ was added to the recombinant cells expressing human CYP24. As expected, M3 was observed as the metabolite (Fig. 2). However, M3 was not detected in the recombinant cells expressing rat CYP24 (data not shown).

Based on these results, the metabolic pathway of F_6-1α,25$(OH)_2D_3$ by human CYP24 is summarized in Fig. 5. First, most of the F_6-1α,25$(OH)_2D_3$ is converted into F_6-1α,23*S*,25$(OH)_3D_3$. The metabolite M4 was also produced as a minor metabolite. The metabolite F_6-1α,23*S*,25$(OH)_3D_3$ was further metabolized to M3 via F_6-23-oxo-1α,25$(OH)_2D_3$. However, rat CYP24 showed no production of M3. In the recombinant cells expressing human CYP24, the conversion ratios at 39 hr from F_6-1α,25$(OH)_2D_3$ to F_6-1α,23*S*,25$(OH)_3D_3$, F_6-23-oxo-1α,25$(OH)_2D_3$, M3 and M4 were 43.2, 6.8, 2.8, and 6.2%, respectively. On the other hand, the conversion ratios were 59.7, 3.9, 0 (less than 0.1), and 3.8% in the recombinant cells expressing rat CYP24.

3.6. GC-MS analysis of the trimethylsilylated derivative of the metabolite M3

Fig. 6 shows the mass spectra of the trimethylsilylated derivatives of F_6-1α,25$(OH)_2D_3$, F_6-1α,23*S*,25$(OH)_3$, 23-oxo-F_6-1α,25$(OH)_2D_3$, and the metabolite M3. The mass spectrum of F_6-1α,25$(OH)_2D_3$ showed the molecular ion at *m/z* 740 $(M)^+$ indicating that three hydroxyl groups of F_6-1α,25$(OH)_2D_3$ at C-1, C-3 and C-25 positions were trimethylsilylated. The trimethylsilylated derivative of F_6-1α,24*R*$(OH)_2D_3$, and those of 1β-epimer and 3α-epimer of F_6-1α,25$(OH)_2D_3$ showed mass spectra similar to that of F_6-1α,25$(OH)_2D_3$ with the molecular ion at *m/z* 740 $(M)^+$ (data not shown). The mass spectrum of F_6-1α,23*S*,25$(OH)_3D_3$ showed the molecular ion at *m/z* 828 $(M)^+$ indicating that the four hydroxyl groups were trimethylsilylated. On the other hand, trimethylsilylated derivative of 23-oxo-F_6-1α,25$(OH)_2D_3$ showed two distinct peaks with retention times at 16.2 min (I) and 16.7 min (II) in GC profile (data not shown). The mass spectrum of the compound I showed the molecular ion at *m/z* 754 $(M)^+$ indicating that three hydroxyl groups of 23-oxo-F_6-1α,25$(OH)_2D_3$ were trimethylsilylated (Fig. 6C). In contrast, the compound II showed the molecular ion at *m/z* 826 $(M)^+$ indicating the presence of four hydroxyl groups (Fig. 6D). This compound appeared to be the trimethylsilylated derivative of the enol form of 23-oxo-F_6-1α,25$(OH)_2D_3$ resulting from keto-enol equilibrium. Although the mass spectrum of M3 was quite similar to

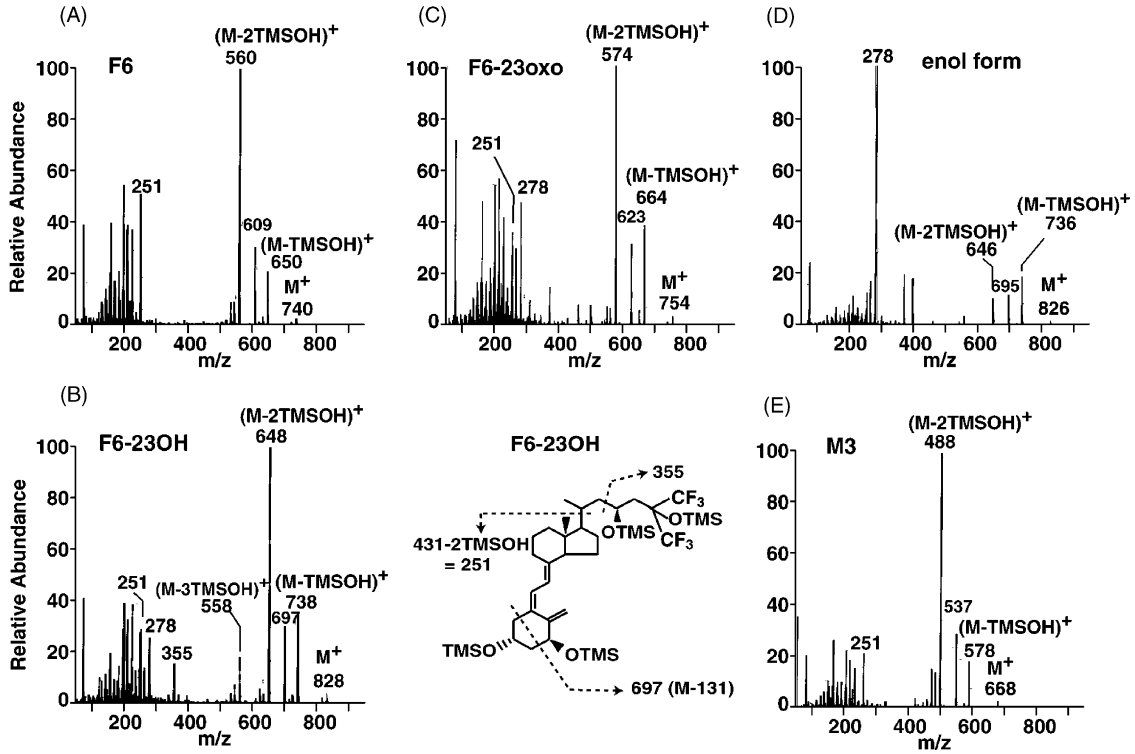

Fig. 6. Mass spectra of trimethylsilylated derivatives of F_6-1α,25(OH)$_2$D$_3$ (A), F_6-1α,23*S*,25(OH)$_3$ (B), 23-oxo-F_6-1α,25(OH)$_2$D$_3$ (C), the putative enol form of 23-oxo-F_6-1α,25(OH)$_2$D$_3$ (D) and the metabolite M3 (E). The experiments were repeated twice.

that of F_6-1α,25(OH)$_2$D$_3$ as shown in Fig. 3, the mass spectrum of the trimethylsilylated derivative of M3 was clearly different from that of F_6-1α,25(OH)$_2$D$_3$. The molecular ion at *m/z* 668 $(M)^+$ indicated that M3 contains two hydroxyl groups. The fact that the fragmentation pattern below *m/z* 251 is similar to that of F_6-1α,25(OH)$_2$D$_3$ strongly suggests that the A ring of M3 contains two hydroxyl groups. Thus, it appeared that side-chain of M3 contains neither hydroxyl nor oxo groups.

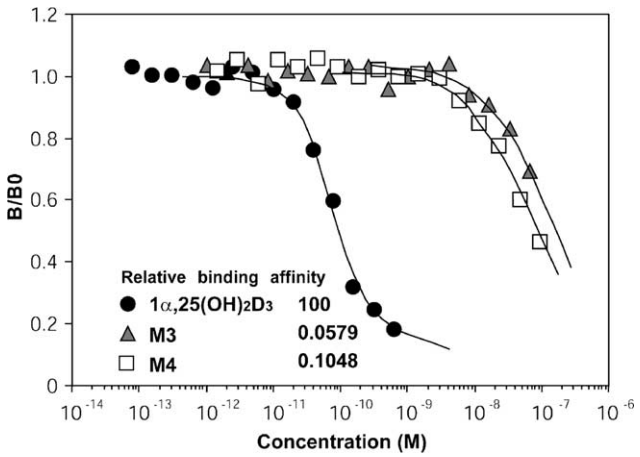

Fig. 7. Displacement of [^{3}H]-1α,25(OH)$_2$D$_3$ from calf-thymus VDR preparation by increasing concentrations of the metabolites M3 (▲), M4 (□) and the control 1α,25(OH)$_2$D$_3$ (●). Molecular weights of M3 and M4 were assumed to be 524 and 356 on the basis of their mass spectra shown in Fig. 3. Assays for each sample were carried out once in duplicate.

3.7. Binding affinity of the metabolites for Vitamin D receptor

The calf-thymus VDR binding assay clearly demonstrated that the metabolites M3 and M4 had much lower affinity for VDR than 1α,25(OH)$_2$D$_3$. The concentrations of 1α,25(OH)$_2$D$_3$, M3 and M4 in the aqueous solution for 50% B/B_0 were 79 pM, 138 nM and 78 nM, respectively. The affinity of the metabolites M3 and M4 for VDR was estimated to be approximately 1/1700 and 1/1000 of 1α,25(OH)$_2$D$_3$, respectively (Fig. 7). Lack of VDR binding indicates that these metabolites are probably inactive but transactivation studies need be performed before the conclusion can be made that they lack biological activity.

4. Discussion

A large number of Vitamin D analogs have been synthesized for clinical applications such as treatment of rickets, osteoporosis, renal osteodystrophy, psoriasis, and secondary hyperparathyroidism as well as prevention of autoimmune diseases and cancer [1]. Structural alterations were distributed over the 1α,25(OH)$_2$D$_3$ molecule. Introduction of fluorine in the side-chain increased the calcemic activity probably by increasing the half-life of the molecule. In the previous study [5], we compared the distribution and metabolism of F_6-1α,25(OH)$_2$D$_3$ and 1α,25(OH)$_2$D$_3$ in bones of rats by autoradiography and radio-HPLC.

In the dosed groups, radioactivity was detected locally in the metaphysis, the modeling site in bones. Compared with the 1α,25(OH)$_2$D$_3$, F$_6$-1α,25(OH)$_2$D$_3$ was significantly retained in this site; moreover, it mainly persisted as unchanged compound and F$_6$-1α,23*S*,25(OH)$_3$D$_3$.

Our previous study using *E. coli* expression system clearly demonstrated that the metabolism of 1α,25(OH)$_2$D$_3$ in target tissues such as the kidneys, the small intestine, and bones mostly depended on CYP24 [11,12]. In this study, we compared the metabolism of F$_6$-1α,25(OH)$_2$D$_3$ in the recombinant *E. coli* cells co-expressing rat CYP24, bovine ADX and ADR with the metabolism in the target tissues of rats. As expected, the conversion of F$_6$-1α,25(OH)$_2$D$_3$ to F$_6$-23-oxo-1α,25(OH)$_2$D$_3$ via F$_6$-1α,23*S*,25(OH)$_3$D$_3$ was clearly demonstrated. The slower conversion rate from F$_6$-1α,23*S*,25(OH)$_3$D$_3$ to F$_6$-23-oxo-1α,25(OH)$_2$D$_3$ than that from F$_6$-1α,25(OH)$_2$D$_3$ to F$_6$-1α,23*S*,25(OH)$_3$D$_3$ caused the accumulation of F$_6$-1α,23*S*,25(OH)$_3$D$_3$. This metabolic pattern is quite similar to that in the target tissues of rats, suggesting that the metabolism of F$_6$-1α,25(OH)$_2$D$_3$ in the target tissues depends on CYP24 [3–5]. In addition to F$_6$-1α,23*S*,25(OH)$_3$D$_3$ and F$_6$-23-oxo-1α,25(OH)$_2$D$_3$, the novel metabolite M4 was observed in this study. After hydrogen abstraction of C-23 position of the substrate, a part of the substrate–radical–intermediate appeared to be converted into the metabolite M4, while most of the substrate–radical–intermediate was converted into the 23-hydroxylated product, F$_6$-1α,23*S*,25(OH)$_3$D$_3$. It is reasonable to assume that radical rearrangement after hydrogen abstraction of the C-23 position produced the metabolite M4 according to the reaction mechanism observed in the oxidation of norcarane by P450cam (CYP101), P450BM-3 (CYP102), CYP2B1 and CYP2E1 [23]. The fact that M4 was produced from F$_6$-1α,25(OH)$_2$D$_3$, but not from F$_6$-1α,23,25(OH)$_3$ or from 23-oxo-F$_6$-1α,25(OH)$_2$D$_3$, was consistent with this assumption. Although the side-chain cleavage might have included the multi-step oxidation, which is observed in CYP51 [24], CYP19 [25] and CYP17 [26], the radical rearrangement mechanism appears to be more reasonable. From the viewpoint of metabolic inactivation of F$_6$-1α,25(OH)$_2$D$_3$, the conversion to M4 appears to be essential because both F$_6$-1α,23*S*,25(OH)$_3$D$_3$ [8] and F$_6$-23-oxo-1α,25(OH)$_2$D$_3$ have affinity for VDR, similar to F$_6$-1α,25(OH)$_2$D$_3$.

Our previous study on rat CYP24 revealed that the enzyme can catalyze six-step monooxygenation from 1α,25(OH)$_2$D$_3$ through 1α,24,25(OH)$_3$D$_3$, 24-oxo-1α,25(OH)$_2$D$_3$, 24-oxo-1α,23,25(OH)$_3$D$_3$, 24,25,26,27-tetranor-1α,23(OH)$_2$D$_3$, and 24,25,26,27-tetranor-23-oxo-1α(OH)D$_3$ to calcitroic acid [11]. This metabolic pathway is designated as C-24 hydroxylation pathway [27,28]. On rat CYP24, almost all metabolites were included in the C-24 hydroxylation pathway. On the other hand, human CYP24 showed both C-24 and C-23 hydroxylation pathways [10,28,29]. Thus, we assumed that human CYP24 might show higher 23*S*-hydroxylation activity towards F$_6$-1α,25(OH)$_2$D$_3$ than rat CYP24. As expected, the V_{max}/K_m value for human CYP24 was 2-fold higher than that for rat CYP24. In addition, the conversion rate in human CYP24-harboring cells from F$_6$-1α,23*S*,25(OH)$_3$D$_3$ to F$_6$-23-oxo-1α,25(OH)$_2$D$_3$ was significantly higher than that in rat CYP24-harboring cells. The conversion from F$_6$-23-oxo-1α,25(OH)$_2$D$_3$ to M3 was not observed in rat CYP24-harboring cells but was observed in human CYP24-harboring cells. As the metabolite M3 showed extremely low affinity for VDR, the conversion of F$_6$-1α,25(OH)$_2$D$_3$ into M3 was considered to be metabolic inactivation of F$_6$-1α,25(OH)$_2$D$_3$. These results clearly indicate species-based difference in CYP24 between humans and rats in the metabolism of F$_6$-1α,25(OH)$_2$D$_3$. GC-MS analysis strongly suggests that M3 contains two hydroxyl groups at 1α and 3β positions, but the side-chain of M3 contains neither hydroxyl nor oxo groups. Based on HPLC, LC-MS and GC-MS analyses, M3 appears to be an ether compound with an ethereal bridge at the C-23 or C-25 position, although the detailed reaction mechanism, including the C–C bond cleavage, is unclear. Tanaka *et al.* [30] reported radical rearrangement in the metabolism of 24-epi-25(OH)D$_2$. Thus, radical rearrangement after hydrogen abstraction, probably at the C-24 position, might be involved. It should be noted that the conversion from 23-oxo-F$_6$-1α,25(OH)$_2$D$_3$ into M3 is not oxidation but reduction, suggesting that this conversion would contain not only CYP24-dependent reaction but also a reduction by an unknown mechanism.

As demonstrated in this study, the metabolism of F$_6$-1α,25(OH)$_2$D$_3$ in the recombinant *E. coli* cells harboring rat CYP24 greatly coincides with the metabolism in rat target tissues [4,5]. This fact suggests that the metabolism of F$_6$-1α,25(OH)$_2$D$_3$ in the recombinant *E. coli* cells harboring human CYP24 would predict its metabolism in human target tissues. Sufficient amounts of the metabolites for HPLC and MS analyses could be readily obtained by the addition of a substrate to the *E. coli* culture. Thus, this recombinant *E. coli* system appears quite useful for predicting the metabolism of Vitamin D analogs in human target tissues before clinical trials.

Acknowledgments

We wish to express our gratitude to Dr. S. Komuro of Sumitomo Chemical Co, Ltd. for useful discussions. This work was supported in part by a Grant-in-Aid for Scientific Research from the Ministry of Education, Science and Culture of Japan.

References

[1] Bouillon R, Okamura WH, Norman AW. Structure–function relationships in the Vitamin D endocrine system. Endocr Rev 1995;16:200–57.

[2] Bishop JE, Collins ED, Okamura WH, Norman AW. Profile of ligand specificity of the Vitamin D binding protein for 1alpha,25-dihydroxyvitamin D_3 and its analogs. J Bone Miner Res 1994;9:1277–88.
[3] Komuro S, Kanamaru H, Nakatsuka I, Yoshitake A, Ishizaki M, Nemoto H, Ueda K, Ebine H, Ninomiya S, Esumi Y. Disposition and metabolism of ST-630 (1) absorption, distribution and excretion after single oral administration of ^{3}H-ST-630 in rats. Xenobio Metabol Dispos 1996;11:505–17.
[4] Komuro S, Kanamaru H, Nakatsuka I, Yoshitake A. Disposition and metabolism of ST-630 (2) metabolism after single oral administration of ^{3}H-ST-630 in rats. Xenobio Metabol Dispos 1996;11:518–29.
[5] Komuro S, Kanamaru H, Nakatsuka I, Yoshitake A. Distribution and metabolism of F_6-1,25$(OH)_2$ Vitamin D_3 and 1α,25$(OH)_2$ Vitamin D_3 in the bones of rats dosed with tritium-labeled compounds. Steroids 1998;63:505–10.
[6] Tanaka Y, DeLuca HF, Kobayashi Y, Ikekawa N. 26,26,26,27,27,27-Hexafluoro-1α,25-dihydroxyvitamin D_3; a highly potent, long-lasting analog of 1α,25-dihydroxyvitamin D_3. Arch Biochem Biophys 1984; 229:348–54.
[7] Okumura H, Yamamuro T, Higuchi S, Harada M, Takamura T, Otomo S, Aihara H, Ikekawa N, Kobayashi T. 26,27-Hexafluoro-1,25-dihydroxyvitamin D_3 prevents osteoporosis induced by immobilization combined with ovariectomy in the rat. Bone Miner 1990;9:101–9.
[8] Kiriyama T, Okamoto S, Ejima E, Kurihara N, Haketa Y, Ito N, Izumi M, Kumegawa M, Nagataki S. Effect of a highly potent fluoro analog of 1,25-dihydroxyvitamin D_3 on human bone-derived cells. Endocrinology 1991;128:81–6.
[9] Honda A, Nakashima N, Shiba Y, Mori Y, Nagata A, Ishizuka S. Modification of 1α,25-dihydroxyvitamin D_3 metabolism by introduction of 26,26,26,27,27,27-hexafluoro atoms in human promyelocytic leukemia (HL-60) cells: isolation and identification of a novel bioactive metabolite 26,26,26,27,27,27-hexafluoro 1α,23(S),25-trihydroxyvitamin D_3. Biochem J 1993;295:509–16.
[10] Hayashi K, Akiyoshi-Shibata M, Sakaki T, Yabusaki Y. Rat CYP24 catalyses 23*S*-hydroxylation of 26,26,26,27,27,27-hexafluorocalcitriol in vitro. Xenobiotica 1998;28:457–63.
[11] Sakaki T, Sawada N, Komai K, Shiozawa S, Yamada S, Yamamoto K, Ohyama Y, Inouye K. Dual metabolic pathway of 25-hydroxyvitamin D_3 catalyzed by human CYP24. Eur J Biochem 2000;267:6158–65.
[12] Sakaki T, Sawada N, Nonaka Y, Ohyama Y, Inouye K. Metabolic studies using recombinant *Escherichia coli* cells producing rat mitochondrial CYP24. Eur J Biochem 1999;262:43–8.
[13] Engstrom GW, Reinnhardt TA, Horst RL. 25-Hydroxyvitamin D_3-23-hydroxylase, a renal enzyme in several animal species. Arch Biochem Biophys 1986;250:86–93.
[14] Pedersen JI, Hagenfeldt Y, Bjorkhem I. Assay and properties of 25-hydroxyvitamin D_3 23-hydroxylase. Biochem J 1988;250:521–6.
[15] Akiyoshi-Shibata M, Sakaki T, Ohyama Y, Noshiro M, Okuda K, Yabusaki Y. Further oxidation of hydroxycalcidiol by calcidiol 24-hydroxylase. Eur J Biochem 1994;224:335–43.
[16] Sakaki T, Sawada N, Takeyama K, Kato S, Inouye K. Enzymatic properties of mouse 25-hydroxyvitamin D_3 1α-hydroxylase expressed in *Escherichia coli*. Eur J Biochem 1999;259:731–8.
[17] Sawada N, Sakaki T, Kitanaka S, Takeyama KI, Kato S, Inouye K. Enzymatic properties of human 25-hydroxyvitamin D_3 1α-hydroxylase. Eur J Biochem 1999;265:950–6.
[18] Blattner FR, Plunkett III G, Bloch CA, Perna NT, Burland V, Rilley M, Vides C, Glasner JD, Rode CK, Mayhew GF, Gregor J, Davis NW, Kirkpatrick HA, Goeden MA, Rose DJ, Mau B, Shao Y. The complete genomesequence of *Escherichia coli* K-12. Science 1997;277:1453–62.
[19] Inouye K, Sakaki T. Enzymatic studies on the key enzymes of Vitamin D metabolism; 1α-hydroxylase (CYP27B1) and 24-hydroxylase (CYP24). Biotechnol Annu Rev 2001;7:179–94.
[20] Nakagawa K, Sowa Y, Kurobe M, Ozono K, Siu-Caldera ML, Reddy GS, Uskokovic MR, Okano T. Differential activities of 1α,25-dihydroxy-16-ene-vitamin D_3 analogs and their 3-epimers on human promyelocytic leukemia (HL-60) cell differentiation and apoptosis. Steroids 2001;66:327–37.
[21] Hiwatashi A, Nishii Y, Ichikawa Y. Purification of cytochrome P-450D1α (25-hydroxyvitamin D_3-1α-hydroxylase) of bovine kidney mitochondria. Biochem Biophys Res Commun 1982;105:320–7.
[22] Lowry OH, Rosebrough NJ, Farr AL, Randall RJ. Protein measurement with the folin phenol reagent. J Biol Chem 1951;193:265–75.
[23] Auclair K, Hu Z, Little DM, Montellano PRO, Groves JT. Revisiting the mechanism of P450 enzymes with the radical clocks norcarane and spiro [2,5] octane. J Am Chem Soc 2002;124:6020–7.
[24] Shyadehi AZ, Lamb DC, Kelly SL, Kelly DE, Schunck WH, Wright JN, Corina D, Akhtar M. The mechanism of the acyl-carbon bond cleavage reaction catalyzed by recombinant sterol 14 alpha-demethylase of *Candida albicans* (other names are: lanosterol 14alpha-demethylase, P-45014DM, and CYP51). J Biol Chem 1996;271:12445–50.
[25] Akhtar M, Calder MR, Corina DL, Wright JN. Mechanistic studies on C-19 demethylation in oestrogen biosynthesis. Biochem J 1982; 20:569–80.
[26] Lee-Robichaud P, Shyadehi AZ, Wright JN, Akhtar ME, Akhtar M. Mechanistic kinship between hydroxylation and desaturation reactions: acyl–carbon bond cleavage promoted by pig and human CYP17 (P-450(17)alpha; 17 alpha-hydroxylase-17,20-lyase). Biochemistry 1995;34:14104–13.
[27] Napoli JL, Pramanik BC, Royal PM, Reinhardt TA, Horst RL. Intestinal synthesis of 24-keto-1,25-dihydroxyvitamin D_3 A metabolite formed in vivo with high affinity for the Vitamin D cytosolic receptor. J Biol Chem 1983;258:9100–7.
[28] Napoli JL, Horst RL. C(24)- and C(23)-oxidation converging pathways of intestinal 1,25-dihydroxyvitamin D_3 metabolism: identification of 24-keto-1,23,25-trihydroxyvitamin D_3. Biochemistry 1983; 22:5848–53.
[29] Beckman MJ, Tadikonda P, Werner E, Prahl J, Yamada S, DeLuca HF. Human 25-hydroxyvitamin D_3-24-hydroxylase, a multicatalytic enzyme. Biochemistry 1996;35:8465–72.
[30] Tanaka Y, Sicinski RR, DeLuca HF, Sai H, Ikekawa N. Unique rearrangement of ergocalciferol side chain in vivo: production of a biologically highly active homologue of 1,25-dihydroxyvitamin D_3. Biochemistry 1986;25:5512–8.